Thermoreversible Gelation and Polymorphic Transformations of Syndiotactic Polystyrene in Toluene and Toluene + Carbon Dioxide Fluid Mixtures at High Pressures

Jian Fang and Erdogan Kiran*

Department of Chemical Engineering, Virginia Polytechnic Institute and State University, Blacksburg, Virginia 24061

Received July 7, 2008; Revised Manuscript Received August 7, 2008

ABSTRACT: The gelation and crystallization processes in solutions of syndiotactic polystyrene in toluene and toluene + carbon dioxide fluid mixtures were studied in a variable-volume view-cell system over a pressure range from 7 to 50 MPa for polymer concentrations up to 25 wt % and for CO_2 concentrations up to 43 wt %. All the solutions in toluene and in toluene + CO_2 mixtures up to 16 wt % CO_2 displayed only a sol−gel boundary. Solutions with 28 wt % CO_2 displayed also a liquid−liquid phase boundary. Solutions in 43% CO_2 displayed instead a fluid−solid crystallization boundary along with a liquid−liquid phase boundary. Consequences of the phase separation path on the eventual morphology and the crystal state of the polymer were investigated. When solutions are cooled to room temperature while maintaining pressure constant during which the sol−gel boundary is crossed first, the resulting morphology is fibrillar and the polymer displays the δ crystal form with a trace amount of the β form. When the solutions are depressurized instead, holding the temperature constant during which liquid−liquid phase boundary is crossed first, with further cooling the polymer-rich phase (PRP) leads to a stacked-lamellar morphology with the β crystal form. The polymer-lean phase (PLP) leads to a mixed morphology with lamellar layers connected with fibrils and the polymer displays a mixed crystal structure consisting of the $\delta + \beta$ polymorphs. In the absence of gelation at high CO_2 levels, the crystallization leads to only the β polymorph. A mechanistic framework is provided to account for the formation of these different polymorphs from the different phase separation paths followed.

Introduction

Syndiotactic polystyrene (sPS) is a polymer of continuing interest due to its high melting temperature, high crystallization rate, and high chemical stability.[1] It has been shown to display a complex crystalline structure with five different polymorphs.[2−4] The α and β forms are all-trans planar zigzag chain conformations, while the γ, δ, and ε forms display 2_1 helical conformations. The δ form refers to clathrate or intercalate cocrystal formed by incorporation of solvent molecules into the crystalline lattice. The γ form is free of solvent molecules in the crystalline lattice, which can be obtained by thermal treatment of the δ form.[5] If the solvent molecules in the δ form are extracted by using boiling acetone[5] or supercritical CO_2,[6] a nanoporous crystalline phase δ_e form, "emptied" δ form, can be generated. Recently, a new crystalline form of sPS, named ε form, has been reported.[7] The ε form is also a nanoporous crystalline phase, in which pore is in "channel" shape instead of the "cavity" shape in δ_e form.[8] Thermodynamically, the all-trans planar zigzag conformation is more stable compared to the helical conformation at ambient conditions. The transformation from the helical form to the all-trans form can be achieved by heating or thermal annealing. The helical δ form can be obtained from solutions in suitable solvents or by sorption of suitable solvents into the amorphous sPS (obtained by rapid quench from melt) or semicrystalline sPS in the α or γ form.[9,10] However, the β form once formed is stable in the presence of solvents and cannot be transformed into the δ form.[11]

The solid−solid crystal form transitions of sPS have also been studied in carbon dioxide at high pressures.[12,13] Carbon dioxide is a well-known plasticizer. Thus polymers can undergo recrytallization at temperatures below their nominal glass transition temperatures. Indeed, it is reported that when exposed to compressed carbon dioxide, sPS undergoes α to β or γ to β transitions in the solid state which otherwise occurs only in the presence of liquid solvents.[12] It is shown that, in the glassy state, sPS can be transformed directly into the γ form when exposed to CO_2 at about 6 MPa and 363 K[12] or above the critical pressure and temperature of carbon dioxide in the pressure range from 8 to 20 MPa and in the temperature range from 308 to 373 K.[13] These observations are interesting in that traditionally the γ form is obtained by treating the glassy sPS with solvents such acetone or tetrachloroethane and then removing the solvent by thermal or vacuum techniques.[12,13] The γ form obtained with exposure to carbon dioxide transforms into the α form at higher temperatures (i.e., 483 K), with a high degree of crystal perfection. If during thermal annealing at temperatures above 483 K the amorphous sPS were to be subjected to carbon dioxide at higher pressures (about 12 MPa), it is reported to directly transform to the β form instead of the α form.[12] The direct transformation to the β form in carbon dioxide is intriguing in that the β form is normally obtainable by slow cooling from the melt, not from the glassy state.

Besides its complex polymorphism, sPS has also been shown to undergo a thermoreversible gel in a variety of solvents.[14−18] Thermoreversible gels are physical gels and differ from chemical gels which are networks formed through covalent bonds and are heat-irreversible. In thermoreversible gels, the networks are formed through van der Waals interactions. The energy associated with these interactions is of the order of κT and thus these gels are thermoreversible.[19] In water, biopolymers often undergo gelation due to hydrogen bonds.[20] Formation of physical gels in synthetic polymers in organic solvents in the absence of hydrogen bonds can arise as a result of phase separation accompanied by vitrification or crystallization, or as a result of formation of "polymer−solvent" compounds.[19,21] Numerous studies on thermoreversible gelation of sPS in different solvents such as chloroform,[15] toluene,[15] benzene,[14] and bromoform[16]

* To whom correspondence should be addressed. E-mail: ekiran@vt.edu. Tel: 540-231-1375. Fax: 540-231-5002.

10.1021/ma801511c CCC: $40.75
Published on Web 09/24/2008

have already been reported. In these gels, the polymer-rich phase is characterized as a "polymer−solvent compound", in which the solvent molecules are included in well-defined positions between sPS chains that are in their 2/1 helical conformation. These gels are reported to be stable and strongly elastic. However, studies with bulky solvents such as octadecyl benzoate[22] and 1-chlorotetradecane[23] have shown that these solvent molecules fail to be incorporated into the cavities created by the helical sPS chain, and in general fail to form a polymer−solvent compound. The gels formed in solutions in bulky solvents give rise to pastelike opaque gels with much lower elasticity. In these systems, the polymer-rich phase is found to display ordered all-trans planar chain conformation instead of 2/1 helical conformation.

The phase behavior of sPS in a series of solvents, including chloroform, chlorobenzene, 1,2-dichlorobenzene, *o*-xylene, 1,2,4-tricholobenzene, and decalin (which represent an order of decreasing solvent quality for sPS), was investigated over the whole polymer concentration range by Berghmans and coworkers[17,18,24,25] using differential scanning calorimetry (DSC). The solvent quality was found to play a significant role. In good solvents, the melting point depression of the β form with planar zigzag conformation was observed to be larger than in poor solvents. However, the stability of the δ form was found to increase with increasing solvent quality. In good solvents, the β form was observed to become the thermodynamically stable phase at high polymer concentrations while the δ form becomes the more stable phase at lower polymer concentrations. In poor solvents, the β form is observed to be the stable phase over the whole polymer concentration range.

The properties of polymeric materials are inherently dependent on their microscopic structure, which is a strong function of their process history. In many cases, phase separation plays a major role. Two modes of phase separation are important for solutions of semicrystalline polymer. These are the liquid−liquid (L−L) and the fluid−solid (F−S) phase separation, i.e., crystallization. In some systems, instead of the whole system undergoing crystallization, gelation is the prevalent phase separation process which involves crystallization of localized domains that act as anchors. Thermally induced phase separation (TIPS) in combination with crystallization is an important technique for the preparation of polymeric porous membranes.[26−28] The process is usually initiated by a thermally induced L−L phase separation, which is then followed by crystallization. The final structure depends on the location of the L−L phase and the F−S (crystallization) phase boundaries. These studies are traditionally carried out at atmospheric pressure. For the solutions of polymers in binary fluid mixtures of an organic solvent with CO_2, the pressure becomes a key tuning parameter to regulate the solvent properties, and consequently the miscibility or phase separation conditions. In these systems, pressure-induced phase separation (PIPS) in combination with crystallization, simply the temperature-induced phase separations that are carried out at high pressures, offers new opportunities to form polymers with unique microstructures. In a recent study, Zhang et al.[29] reported the morphology of polyethylene crystals formed in *n*-pentane solutions at high pressures. Different morphologies are displayed depending upon the phase separation paths employed and whether or not crystallization is induced directly by crossing the F−S boundary by cooling at high pressure, or is induced by a liquid−liquid phase separation first via a pressure quench which is then followed by cooling to cross the L−S phase boundary.

In the present study, we have investigated the gelation or crystallization process for sPS in toluene and toluene + CO_2 mixtures at high pressures. We are now reporting the phase behavior for these solutions as a function of pressure (up to 50 MPa), polymer concentration (up to 25%), and CO_2 content (up to 43%) in the fluid mixtures. The morphology and the crystal habits that are generated by sPS samples after constant pressure cooling, or constant temperature pressure quench followed by cooling are characterized by XRD, SEM, DSC, and FTIR. The results are discussed in terms of the different paths that are followed. The results are also compared with the ambient pressure phase behavior of sPS in toluene that has been reported in the literature.[15,30] Toluene is known to be a good solvent for sPS. The addition of CO_2 to toluene that is now being presented provides an opportunity to investigate the influence of controlled changes in the solvent quality that can be achieved by adjusting either the pressure, or the temperature, or the amount of CO_2 in the fluid mixture and its consequences in the phase behavior, and the polymer crystal forms that are promoted.

Experimental Section

Materials. The syndiotactic polystyrene (with 98% syndiotactic triads) was purchased from Scientific Polymer Products Inc. The polymer had a weight average molecular weight of $M_w = 3.2 \times 10^5$ g/mol and a polydispersity of $M_w/M_n = 3.9$. The solvent, toluene, with a minimum purity of 99.9% was purchased from AlliedSignal. Carbon dioxide with a minimum purity of 99.99% was purchased from Air Products. The polymer and the solvents were used as received.

Experimental System. Experiments were carried out in a variable-volume view-cell system described in our earlier publications.[31] The cell is equipped with two sapphire windows permitting either visual or optical observations. The cell is heated by four cartridge heating elements. A movable piston coupled with a pressure generator is used to alter the inner volume of the cell and thereby adjust the system pressure. It is operable at pressures up to 70 MPa and temperatures up to 473 K. An optical fiber illuminator is used as the light source and the transmitted light intensity is monitored with a fast response photodiode detector. During phase boundary determination, the temperature, pressure, and transmitted light intensities are recorded in real time with a dedicated computer.

Experimental Procedures. In a typical experiment, an accurately weighed amount of polymer is first loaded into the cell. This is followed by the addition of a measured amount of the liquid solvent, i.e., toluene. The cell is then sealed and connected to the CO_2 charge line and the pressure generator. For experiments involving binary fluid mixtures of toluene + CO_2, carbon dioxide is charged from a preloaded high-pressure transfer vessel. The amount of carbon dioxide charged is assessed from the change in the mass of the transfer vessel. After the loading process is completed, the cell temperature and pressure are brought to the desired conditions for dissolution of polymer, forming a homogeneous solution. The miscibility is visually verified through the sapphire windows. A magnetic stirrer is used to facilitate the dissolution process.

Figure 1a describes the paths that were followed in determination of phase boundaries. Phase boundaries were approached either by lowering the temperature while keeping the pressure constant (Path 1) or by lowering the pressure while keeping the temperature constant (Path 2). In experiments where temperature was lowered along Path 1, pressure was adjusted with the aid of the pressure generator to compensate for the volumetric change that accompanies temperature reduction and thus maintain constant pressure conditions. From measurements of the temperature, pressure, and the transmitted light intensities (I_{tr}), graphs depicting the changes in the transmitted light intensity with temperature (along a constant pressure path, Path 1) or with pressure (along a constant temperature path, Path 2) are generated. These are shown in Figure 1b. In these plots, the temperature or the pressure corresponding to the departure from the baseline for I_{tr} is identified as the phase separation temperature or pressure. In the present study, the majority of experiments were conducted along Path 1 at different pressures to determine the fluid−solid or the sol−gel phase boundary that is associated with the crystallization or the gelation of sPS. Once the phase-separated regions were entered, phase boundaries were again

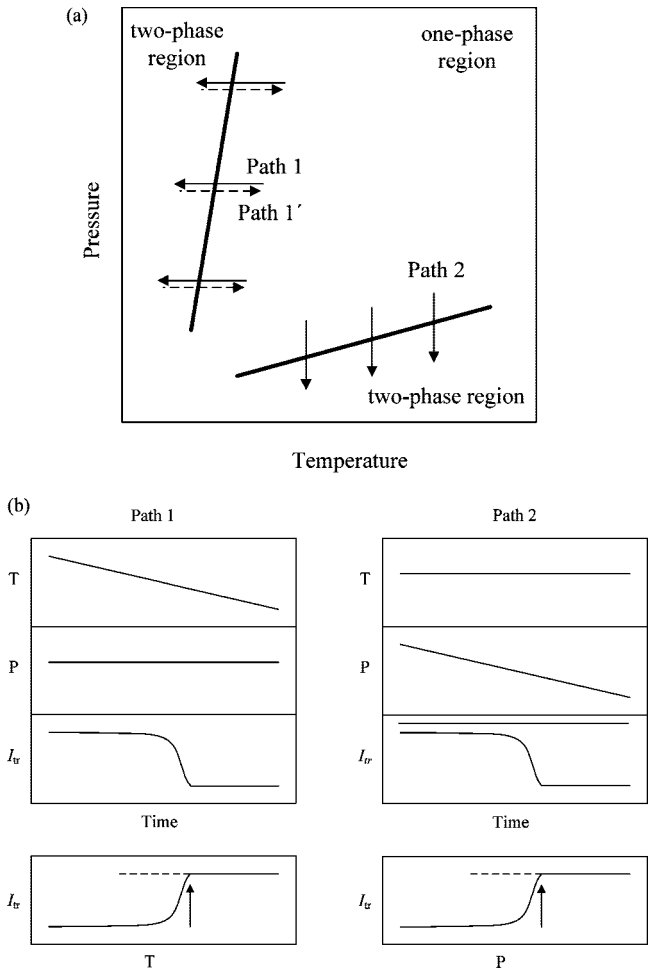

Figure 1. Schematic representation of different paths followed to determine the phase boundaries and the corresponding changes in T, P, and I_{tr} with time.

determined, but this time in the reverse direction by increasing the temperature (labeled as Path 1′ in the figure). In the reverse direction, what is determined is either the melting (S−F) transition for the crystals or the gel−sol transition.

The distinction between gelation and crystallization was made by visual observations. While in systems that undergo crystallization magnetic stirrer motion remains free, when gelation occurs, it gets stuck in the gel and stops turning. Along Path 1, whenever the gelation occurred during cooling to ambient temperature, the system was held for an additional 24 h at the ambient temperature at high pressure to mature the gel. After this maturation time the cell was depressurized and opened to collect the wet gel. Along Path 2, after the pressure-induced L−L phase separation the cell was cooled to ambient temperature while allowing the pressure to decrease, without any further adjustment of the pressure. As before, the system was held for an additional 24 h to mature the gel at the ambient temperature and the prevailing lowered pressure. After final depressurization to ambient pressure and opening the cell, samples were collected from the upper (representing the polymer-lean phase) and the lower (representing the polymer-rich phase) layers of the cell cavity. The wet gels thus collected were air-dried by exposing to open air flow in a hood for 24 h for natural evaporation of the solvent. For some of the samples drying was also carried out by extracting the wet gel with supercritical carbon dioxide at 313 K and 21 MPa for 24 h.

Characterizations by FTIR, SEM, and DSC. IR characterizations were carried out with an FTS 3100 (Digilab) FTIR spectrometer. The resolution was 2 cm^{-1} and 32 scans were co-added to obtain a spectrum for each sample. The air-dried gels or crystals were mixed with KBr powder. The transmission spectra were obtained from these prepared KBr disks.

A Leo 1550 field emission scanning electron microscope (FESEM) was used to examine the morphology of the gels or crystals. The air-dried gel samples were freeze-fractured after immersing in liquid nitrogen. A 15 nm layer of gold was coated on the samples using a Cressington 208 HR sputter coater to reduce electron charging effects. The morphological features of fractured cross-sectional surfaces were investigated.

X-ray diffraction (XRD) patterns of vacuum-dried polymer samples were obtained with a Scintag XDS-2000 powder diffractometer operated at 45 kV and 40 mA using Cu Kα monochromatized radiation ($\lambda = 0.154\ 178$ nm).

The thermal behavior of the gels or crystals was investigated using a Perkin Elemer (Pyris Diamond) differential scanning calorimeter. Due to the presence of the resident solvent in the air-dried gels, gold-plated stainless-steel high-pressure capsules were used as sample holders to prevent solvent loss during scans. Thermograms were recorded at heating or cooling rates at 10 K/min in the temperature range 313−523 K.

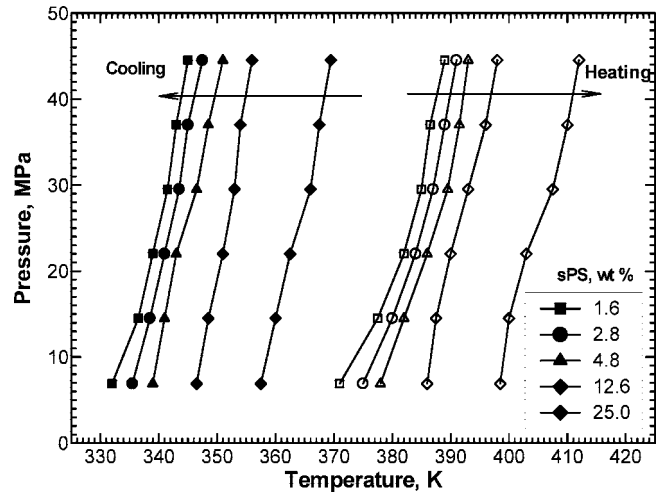

Figure 2. Sol−gel phase boundaries for syndiotactic polystyrene solutions in toluene at different polymer concentrations. Filled symbols represent the gel formation points upon cooling and opened symbols represent the gel melting points upon heating.

Results and Discussion

1. Phase Boundaries. *1.1. sPS + Toluene.* Figure 2 shows the phase boundaries determined under constant pressure cooling and heating experiments (Path 1 and Path 1′ in Figure 1) in 1.6, 2.8, 4.8, 12.6, and 25.0 wt % solutions of sPS in pure toluene. The experiments were carried out by maintaining the pressure constant at 6.9, 14.5, 22.0, 29.5, 37.0, and 45.5 MPa. The phase transitions were identified as the sol−gel (Path 1) or the gel−sol (Path 1′) transitions by visual observation. The magnetic stirrer inside the cell is frozen when the sol−gel phase boundary is crossed but becomes free after crossing the gel−sol phase boundary. As shown in Figure 2, the sol−gel and the gel−sol phase boundaries are shifted to higher temperature region with increasing polymer concentration in the solutions. Daniel et al.[15] studied the temperature−concentration phase diagram for sPS + toluene at ambient pressure using DSC measurement. Their results have shown that the melting temperatures of the gels increase from around 373 to 423 K when polymer concentration increases from ∼4 to ∼50 wt %. The gel−sol phase boundaries in the present study are in good agreement with the DSC data reported in the literature. Indeed, while for the 4.8 wt % solution the transitions occur in the temperature region from 378 to 390 K, for 25 wt % solution the range is 399−412 K.

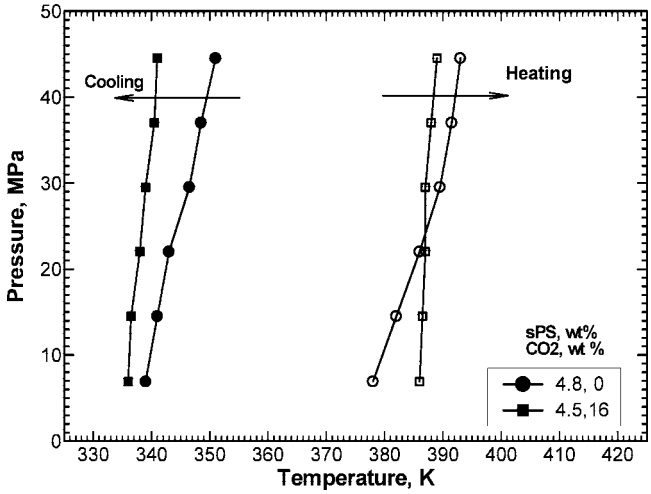

Figure 3. Sol−gel phase boundaries for syndiotactic polystyrene solutions in pure toluene and toluene + CO_2 mixture with 16% CO_2 in the solvent mixture. Filled symbols represent the gel formation points upon cooling and open symbols represent the gel melting points upon heating.

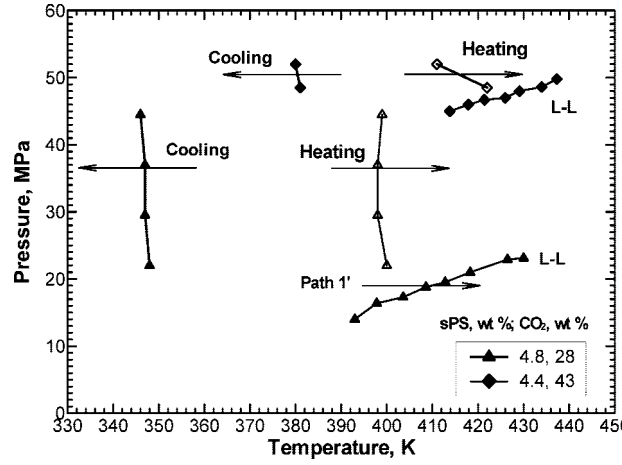

Figure 4. Sol−gel and L−L phase boundaries for syndiotactic polystyrene solutions in toluene + CO_2 mixture with 28% CO_2 and fluid−solid and L−L phase boundaries in toluene + CO_2 mixture with 43 wt % CO_2 in the solvent mixture. Open symbols represent the gel melting (28% CO_2) or crystalline melting (43% CO_2) points upon heating.

Figure 2 shows that the temperature difference between sol−gel (gelation) and gel−sol (redissolution) phase boundary is over 40 K in these solutions. Large hysteresis in solid−fluid transition temperatures is not uncommon and was also reported for crystallization and melting transitions of polyethylene in high pressure *n*-pentane solutions[32] where a 15 K difference was observed. The very large difference between gelation (during cooling) and gel melting (during reheating) observed in present study may arise from the long induction time needed in forming sPS helix conformation for gelation to occur starting from the random sPS coils in solution. Long induction times for coil-to-helix transformation during gelation of sPS in bromoform solution has been discussed in the literature.[16] Berghmans and Deberdt[33] studied the phase behavior of sPS in decalin and in *o*-xylene. The temperatures for formation and melting of helix conformation (δ form) and the zigzag conformation (β form) have been measured by DSC over the whole polymer concentration range. They report a larger temperature difference for the formation and remelting of helix conformation (representing gelation and redissolution) than for the formation (crystallization) and remelting of the zigzag conformation. More recently, an extremely large hysteresis (about 100 K) between gelation and redissolution has been reported for gelation of poly(9,9′-dioctylfluorene) in toluene.[34]

Additional experiments were also carried out along constant temperature paths (Path 2) at selected temperatures higher than gel−sol phase transition temperatures. However, in these experiments in toluene the system remained as homogeneous solutions and no liquid−liquid phase separation was detected.

1.2. sPS + Toluene + CO_2. The influence of CO_2 on the phase boundaries was investigated by adding the CO_2 into sPS solution in toluene. The polymer concentration was at nominal concentration of 4.5 wt % and the compositions of CO_2 in fluid mixture were varied from 0 to 43 wt %.

Figure 3 shows the phase boundaries for 4.5 wt % sPS solution in toluene + CO_2 mixture containing 16 wt % CO_2. The phase boundaries for 4.8 wt % sPS solution in pure toluene (0 wt % CO_2) are also included for comparison. As shown in the figure, the sol−gel boundary is shifted to lower temperatures with addition of 16 wt % CO_2. That the addition of CO_2 lowers the fluid−solid transition temperatures was also observed in poly(4-methyl-1-pentene) (P4MP1) solutions in *n*-pentane + CO_2 (up to 20 wt % CO_2 in the solvent mixtures).[31] The sol−gel or fluid−solid transition temperatures measured in the view cell are the phenomenological observations that reflect the outcome of thermodynamic and kinetic factors for polymer gelation or crystallization which are far from their equilibrium values. Thermodynamically, upon addition of a poor solvent, such as CO_2, the solvent quality of the fluid mixture of toluene + CO_2 for sPS is decreased as compared to the pure toluene. The decreased solvent quality in turn decreases the stability of δ form, and as a result the sol−gel phase boundary corresponding to the formation of δ form (polymer−solvent compound) and the gelation is observed to shift to lower temperatures. Kinetically, for sPS solution in the solvent mixture with 16 wt % CO_2, the rate of toluene intercalation leading to polymer−solvent compound is hindered due to the presence of CO_2, and gelation process is slowed down, thus also shifting the observed sol−gel transition to lower temperatures. Figure 3 suggests that the extent of hindrance to gelation of sPS in toluene is greater at higher pressures. Figure 3 shows the temperature difference between the sol−gel and the gel−sol phase boundaries for solution with 16 wt % CO_2 is 10 K larger than that for the solution in pure toluene. The augmented hysteresis in solution contain CO_2 is consistent with the notion that CO_2 delays the development of the helical conformation leading to gelation.

The temperature−pressure phase diagrams of 4.8 wt % sPS solution in toluene + CO_2 mixture containing 28 wt % CO_2 and 4.4 wt % sPS solution in toluene + CO_2 mixture containing 43 wt % CO_2 are shown in Figure 4. Instead of being at lower temperatures, the sol−gel phase transitions in sPS solution with 28 wt % CO_2 occur at higher temperatures when compared with the solutions in pure toluene and in fluid mixture of 84 wt % toluene + 16 wt % CO_2. The observed phase transition occurring at a higher temperature can be attributed to the appearance of the β form upon cooling. As more CO_2 loaded into system, the solvent quality for sPS becomes poorer. Eventually, the β phase becomes the more stable form than the δ form over the whole polymer concentration range, and the cooling leads to the transition of the solution to the β form at high temperatures. The transition of the solution to the β form is observed at higher temperatures for the sPS solution containing 43 wt % CO_2 in the solvent. This is in accord with the observation that the melting point depression of β form is decreased as the solvent quality becomes even poorer with further addition of CO_2. Another striking difference in the phase diagram shown in Figure 4 is the appearance of the LCST-type liquid−liquid phase boundaries. As would be expected with lowered solvent power,[35]

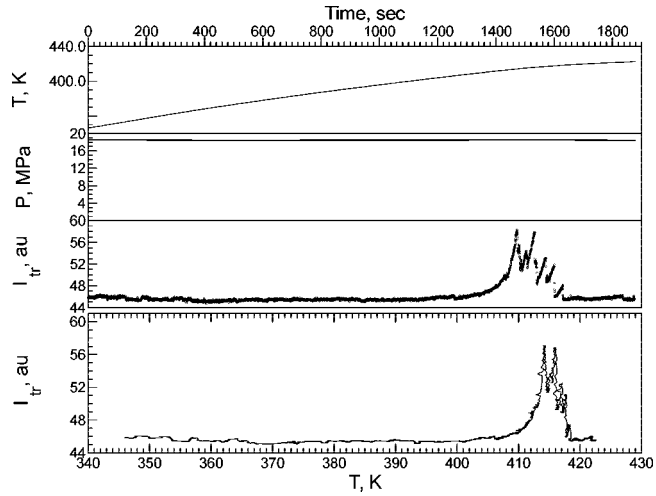

Figure 5. Variation of temperature T, pressure P, and transmitted light intensity I_{tr} with time and I_{tr} with temperature along the constant pressure heating path (as indicated as path B′ in Figure 4) in 4.8 wt % sPS solution in 72 wt % toluene + 28 wt % CO_2 at 18.5 MPa.

the L−L phase boundary shifts to much higher pressures when CO_2 amount in the solution is increased from 28 to 43 wt %.

A special heating experiment was carried out for the 4.8 wt % sPS solution in a fluid mixture of toluene (72) + CO_2 (28) following a constant pressure path (as indicated as Path 1′ in Figure 4). In these experiments, the system was first cooled down to a low temperature below the sol−gel phase boundary to induce gelation. Then it was reheated while maintaining the pressure constant at 18.5 MPa. As predicted by the phase diagram, the system was observed to first go through the gel−sol phase boundary undergoing redissolution and thus entering the homogeneous region. With further heating, this was followed by a re-entry into a heterogeneous two-phase region, but this time due to the liquid−liquid phase separation taking place at the higher temperatures (which is typical of systems showing LCST). The transmitted light intensity was monitored during the whole experiment and is shown in Figure 5. As shown, initially the transmitted light intensity increases as the gel dissolves and the system becomes transparent. But with continued increase in the temperature, as the liquid−liquid boundary is approached and entered, the new phase domains that develop intermittently block or move away from the light path, leading to the observed series of decrease and increase in I_{tr}. As the phase separation progresses further, the light passage is eventually all hindered and the fluctuations die out as reflected by the lowered I_{tr}.

2. Crystal Structure. FTIR spectroscopy has proven to be a powerful technique to distinguish the different polymorphic forms for sPS.[36−40] There are significant differences in absorption spectrum of the samples whether the planar zigzag form or the 2_1 helix is present.[37,39] The planar zigzag form shows the characteristic bands at 1349, 1224, and 537 cm^{-1}, while the 2_1 helix form shows the characteristic bands at 943, 934, 572, and 502 cm^{-1}. Figure 6 shows the FTIR spectra in the range of 800−1400 cm^{-1} of sPS gel samples formed at 44.5 MPa from different solutions at different polymer concentrations. These spectra are similar to each other. The appearance of characteristic doublet bands at 943 and 934 cm^{-1} (highlighted by arrows in the figure) indicates helical conformation and that the formation of δ form which incorporates the solvent molecules in these samples.

3. Morphology. Figure 7 shows the FESEM images of the gels (after air-drying and freeze-fracturing) obtained along Path 1 (constant pressure cooling to room temperature and then

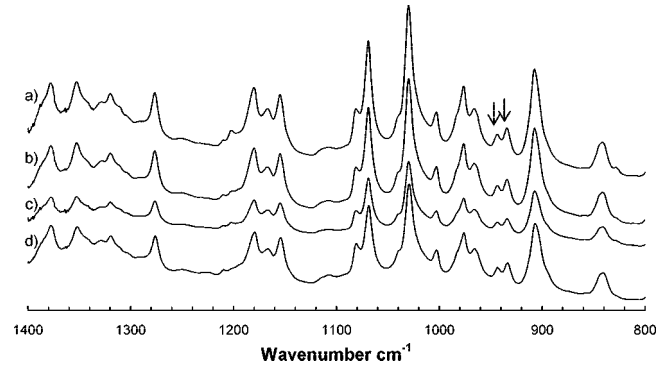

Figure 6. FTIR spectra of syndiotactic polystyrene (sPS) gel samples collected from sPS solutions in pure toluene with different polymer concentrations: (a) 2.8 wt %, (b) 4.8 wt %, (c) 12.6 wt %, and (d) 25.0 wt %.

depressurization) from 1.6, 2.8 12.6, and 25.0 wt % solutions in pure toluene at 44.5 MPa. As shown in the figure, the basic common feature of these gels is a fibrillar network. The network is observed to become denser in gels formed from solutions with increasing polymer concentration reflecting the increased amount of polymer in the gels.

In order to investigate the influence of the method of removal of the solvent from the gel, supercritical CO_2 extraction was also utilized for gels obtained from 4.8% solutions. The formation of aerogels of sPS by supercritical extraction of traditionally prepared gels has already been reported in the literature.[23] Figure 8 shows the comparison of the morphological features of these sPS gel samples which were air-dried, or dried by supercritical CO_2 at 313 K and 21 MPa for 24 h. They both show a fibrillar network structure with fiber diameters in the range of 20−30 nm. However, compared to the air-dried sample, the sample after supercritical CO_2 extraction shows a much finer porous structures, which may be viewed as representing the pore structure of the fresh wet gel. Extraction with supercritical fluids is a well recognized technique to alleviate interfacial tension effects and prevent cell collapse during drying.

4. Path Dependence of the Gel Structure. Figure 9 shows the two different paths for collection of the sPS samples at point B starting from a homogeneous solution at point A. Path 1 is bringing the system into sol−gel phase separated region at constant pressure as a first step which is then followed by a depressurization process. In the second path, the system is first subjected to a pressure quench into L−L phase separation region upon which the solution phase separates into a polymer-rich and a polymer-lean phase which are then cooled to ambient temperature and depressurized.

The X-ray diffraction patterns for the samples collected at point B following such paths from 4.8 wt % sPS solution containing 28 wt % CO_2 are shown in Figure 10. The sPS sample after Path 1displays (Figure 10a) the typical of δ form, as indicated by the diffraction peaks at $2\theta = 8.0°$, 10.3°, 13.5°, 17.3°, 20.1°, 23.4°, and 28.0°.[5] The X-ray diffraction profile changes dramatically for the sample originating from the polymer-rich phase after Path 2 (Figure 10c), which only displays the typical β form indicated by the appearance of the reflections at $2\theta = 6.2°$, 10.4°, 12.3°, 13.6°, 18.6°, and 21.1°.[3] The appearance of the both diffraction peaks corresponding to the δ and β forms in the X-ray diffraction pattern for the polymer-lean phase sample after Path 2, as shown in Figure 10b, indicates the formation of the mixed $\beta + \delta$ crystal forms in this sample. (The XRD spectrum shown in Figure 10d is that of a sample obtained from a solution containing 43% CO_2 and will be discussed later in this section).

Figure 11 shows the FTIR spectra for these samples collected at point B from 4.8 wt % sPS solution in a fluid mixture of

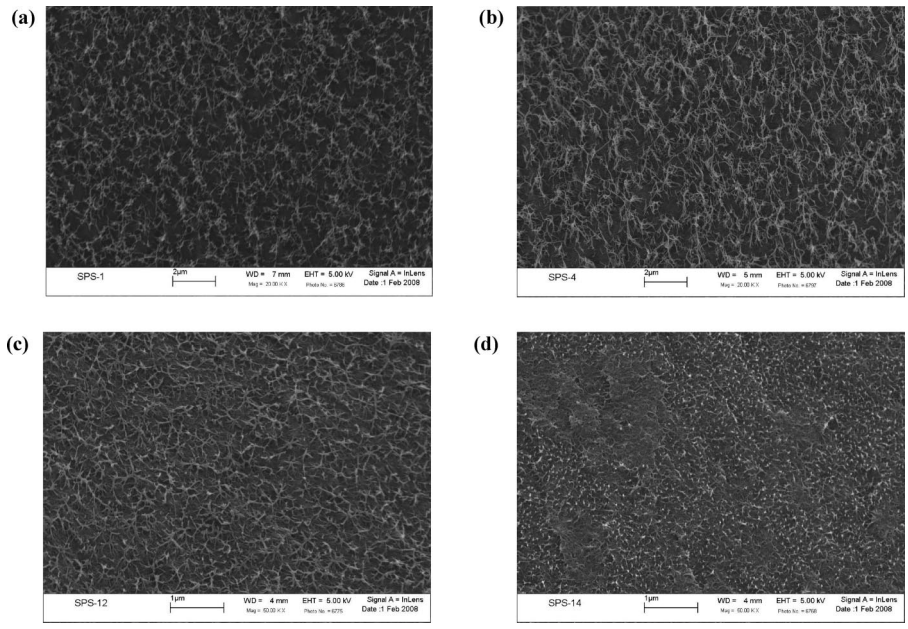

Figure 7. FESEM micrographs of sPS gel samples that were formed at 298 K and 44.5 MPa from the solutions with different polymer concentrations: (a) 1.6 wt %, (b) 2.8 wt %, (c) 12.6 wt %, and (d) 25.0 wt %. The scale bars are 2 μm in (a) and (b) with the magnification of 20 000×; and 1 μm in (c) and (d) with the magnification of 50 000×.

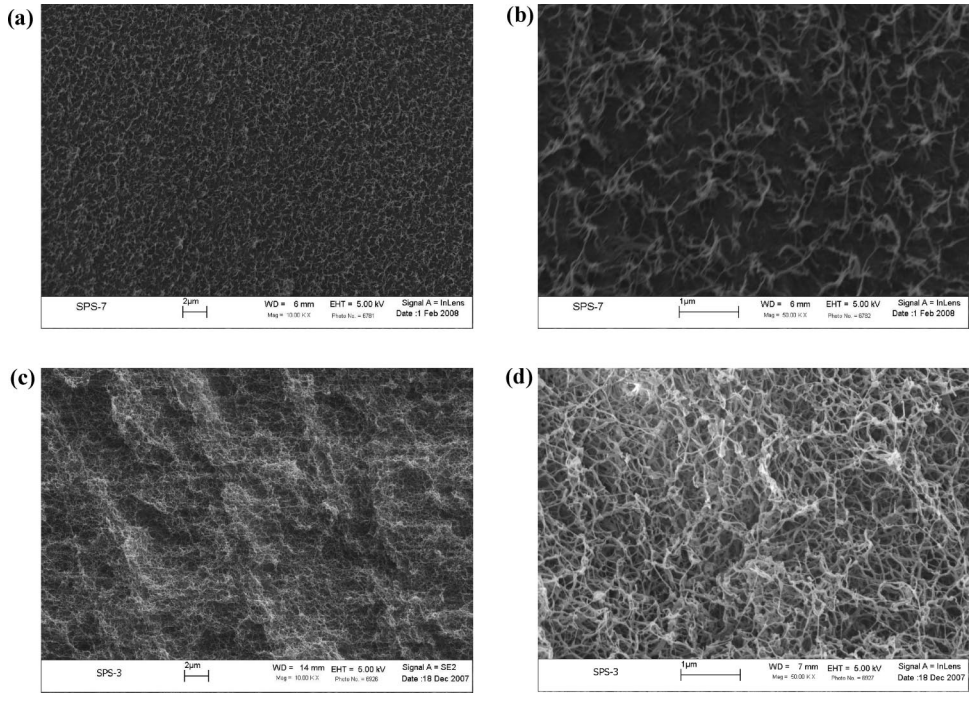

Figure 8. FESEM micrographs of sPS gel samples that were formed at 298 K and 44.5 MPa from the 4.8 wt % solution in pure toluene: (a, b) after air-dried; and (c, d) after 24 h supercritical CO_2 extraction at 313 K and 21 MPa. The scale bars are 2 μm in (a) and (c) with 10 000×; and 1 μm in (b) and (d) with 50 000×.

toluene (72) + CO_2 (28) following these paths. The characteristic doublet peaks at 943 and 934 cm^{-1} correspond to the helical conformation and thus the IR spectrum indicates δ form for the sample obtained from Path 1. The intensities of these peaks are altered as Path 1 is changed to Path 2. The peak intensities are lowered for the sample from the polymer-lean phase and disappear for the sample from the polymer-rich phase that is generated following Path 2. The appearance of the peak at 1222 cm^{-1} and the shoulder peak at 911 cm^{-1} in the spectrum of the sample from the polymer-rich phase indicates the presence of the planar zigzag β form.[25] The intensities of these peaks are observed to decrease in the sample from the polymer-lean phase. These peaks that are characteristic of the β form are absent in the sample from Path 1. As shown in Figure 11, while only the δ form is observed in the sample from Path 1 and the β form is observed in the sample from the polymer-rich phase in Path 2, the polymer-lean phase in Path 2 leads to a mixture of δ and β forms. These results are consistent with the results from the XRD measurements discussed above.

Similar observation can be deduced from analysis of the DSC scans (obtained at 10 K/min) of these three samples illustrated in Figure 12. The DSC scans of the samples with δ form (Path 1 and Path 2 polymer-lean phase) show a broad endothermic peak in the temperature range 353−473 K. This is a typical

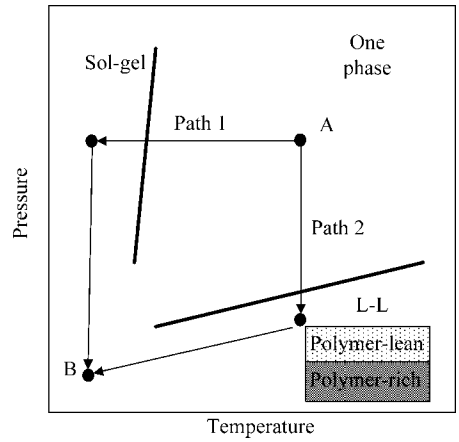

Figure 9. Schematic representation of two different phase separation pathways on a $T-P$ phase diagram. Path 1: constant pressure cooling process to room temperature followed by further depressurization. Path 2: a pressure quench into L−L phase separation region at a given temperature followed by further cooling to room temperature.

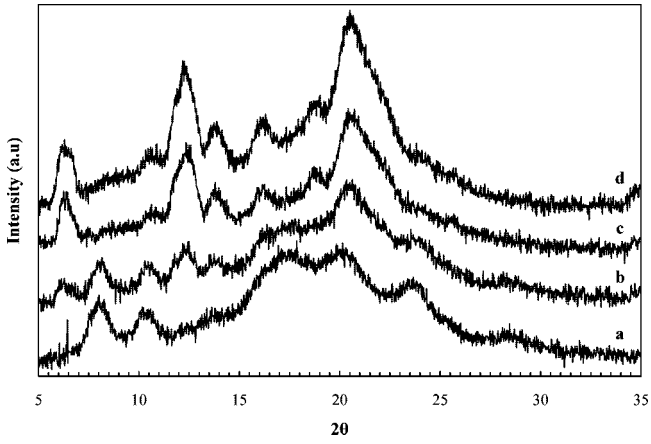

Figure 10. X-ray diffraction patterns in the 2θ range 5°−35° for syndiotactic polystyrene (sPS) samples collected from 4.8 wt % sPS solutions in 72 wt % toluene + 28 wt % CO_2 solution: (a) Path 1; (b) Path 2 polymer-lean phase; (c) Path 2 polymer-rich phase. The XRD pattern shown in (d) is of a sample collected from the polymer-rich phase after Path 2 in a 4.4 wt % solution with higher (43%) CO_2.

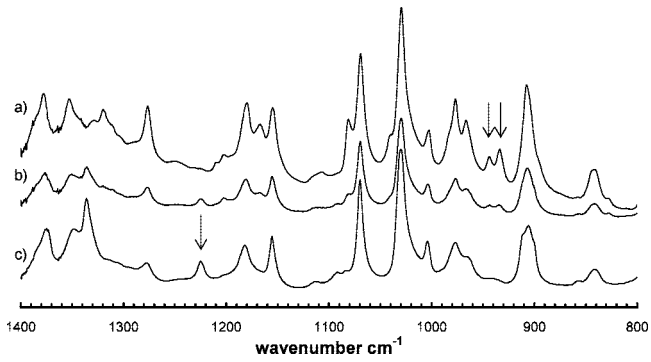

Figure 11. FTIR spectra of syndiotactic polystyrene (sPS) samples collected from 4.8 wt % sPS solutions in 72 wt % toluene + 28 wt % CO_2 solution: (a) Path 1; (b) Path 2 polymer-lean phase; (c) Path 2 polymer-rich phase.

feature reported in the literature for the δ form in the presence of a guest solvent for which the boiling point is in the range of 373−423 K.[41,42] Toluene is in this range with a normal boiling point of 383.6 K. The transformation peaks from δ to γ, and from the γ to α forms are usually masked by the gradual evaporation of the solvent during the scan. The transition from

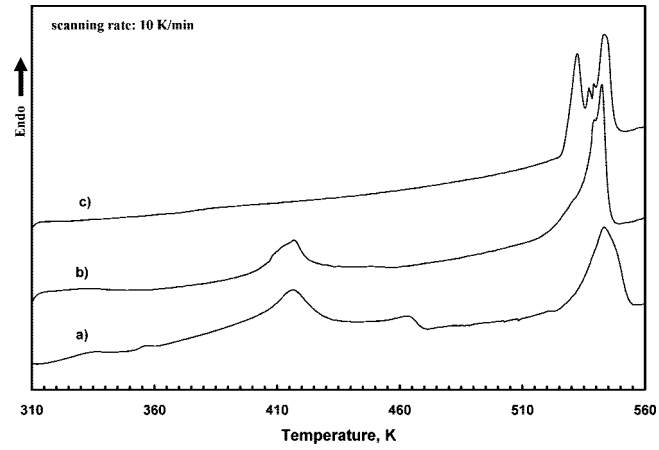

Figure 12. Comparison of the DSC scans for sPS samples from 4.8% solutions in 72 wt % toluene + 28 wt % CO_2: (a) samples collected through Path 1; (b) samples collected from the polymer-lean phase through Path 2; and (c) samples collected from the polymer-rich phase through Path 2.

δ to γ form in a DSC scan is reported to be more apparent for higher boiling point solvents.[43] The DSC scan of the sample showing the planar zigzag β form displays only the endothermic melting peaks at temperature greater than 523 K corresponding to the crystalline melting of the β form. The multiplicity of the melting peaks for polymer crystals formed from high-pressure solutions is common and is often attributed to the multiplicity of the crystal sizes formed in the process as discussed earlier in connection with the crystallization of polyolefins from high-pressure solutions.[29,35]

The morphology of sPS samples collected through Path 1, as shown in Figure 13a, is a fibrillar network structure which is very similar to the sPS gel structure formed from pure toluene solution, as shown in Figure 7. However, a closer examination of Figure 13a indicates the presence of aggregates of lamellar structures corresponding to the β form, dispersed within the fibrillar network. This is more clearly illustrated in Figure 13b, which is an enlargement of the small framed area of Figure 13a. The appearance of the β form dispersed in the δ form in the gel samples, even though the portion is relatively small and not detected in the XRD or IR spectra, is a good indicator of the trend that the β form is beginning to become the more stable crystal form as solvent quality becomes poorer with the addition of more CO_2. The presence of the β form in this sample can also account for the observation of the sol−gel phase transition occurring at higher temperatures compared to the sPS solutions in pure toluene, or in fluid mixtures with lower (i.e., 16 wt %) CO_2 content. Figure 13c shows the sPS samples recovered from polymer-rich phase after Path 2. Instead of a fibrillar network, a strikingly different morphology, lamellar-disk structures, that is indicative of chain-folded crystals is displayed. The fibrillar network is the typical feature for sPS gels that are generated via formation of the "polymer−solvent compound" which prevents chain folding. In contrast, the lamellar structure is the typical chain folded crystal morphology arising from the planar zigzag chain conformation.

The morphology of the sample from the polymer-lean phase from Path 2 is shown in Figure 13d. A combination of high levels of both fibrillar and lamellar structures is displayed. The lamellar layers corresponding to the β form are actually interconnected by fine fibers corresponding to the δ form. These FESEM observations are in good agreement with the XRD, FTIR and DSC results.

The micrograph of sPS samples collected from the polymer-rich phase after Path 2 in a mixture of toluene (57) + CO_2 (43) is shown in Figure 14. The morphology generated from this

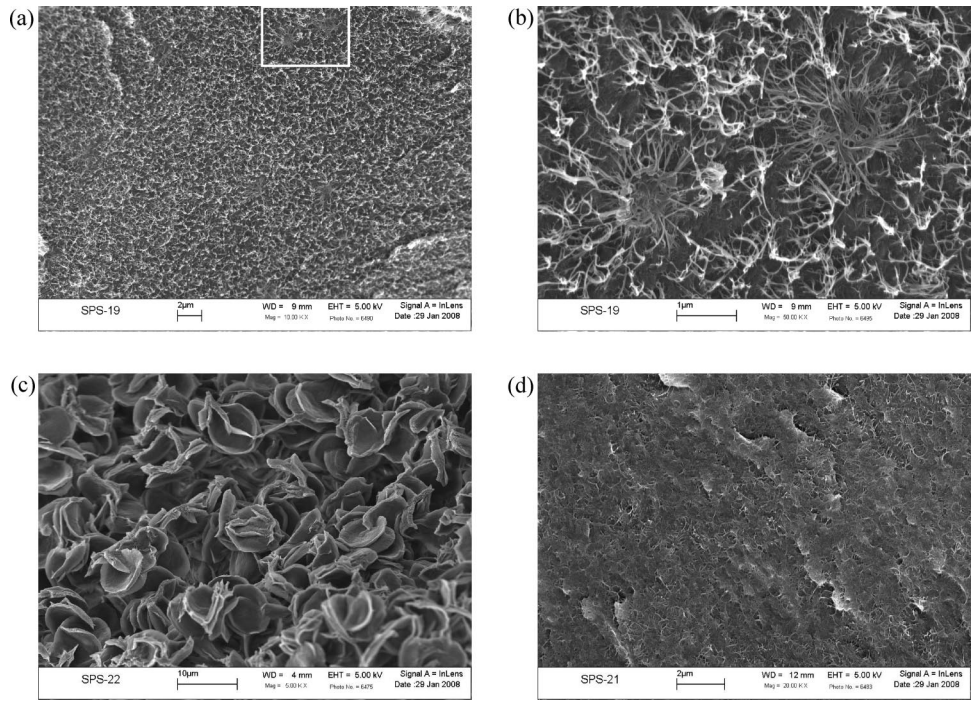

Figure 13. FESEM micrographs of sPS samples that were collected from 4.8 wt % sPS solutions in 72 wt % toluene + 28 wt % CO_2 solution after: (a) Path 1; (b) enlarged area of (a); (c) Path 2, polymer-rich phase; (d) Path 2, polymer-lean phase. The scale bars and magnifications are (a) 2 μm, 10 000×; (b)1 μm, 50 000×; (c) 10 μm, 5000×; and (d) 2 μm, 20 000×.

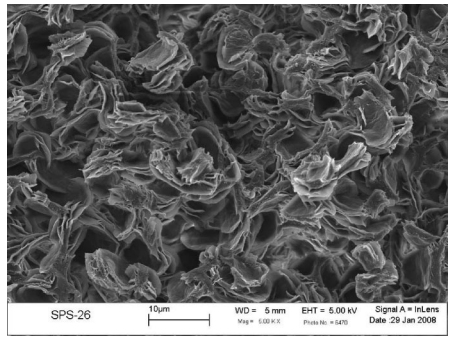

Figure 14. FESEM micrographs of sPS samples that were collected from 4.4 wt % sPS solutions in 57 wt % toluene + 43 wt % CO_2 after Path 2, polymer-rich phase. The scale bar and magnification are 10 μm, 5000×.

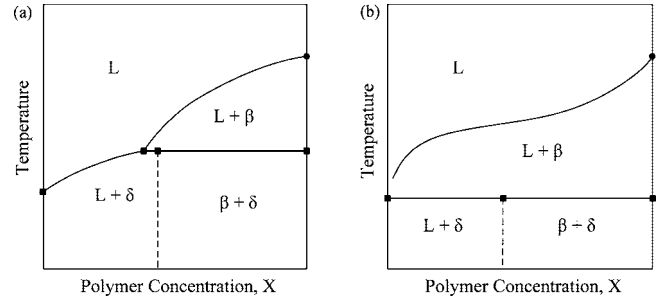

Figure 15. Schematic representation of temperature−concentration phase diagrams for sPS in good (a) and poor (b) solvents at ambient pressure: L, liquid phase; β, β crystal form of sPS; δ, δ crystal form.

solution with much higher carbon dioxide content (43 vs 28%) displays denser stacked-lamellar structures with spherulitic attributes. The XRD diffraction pattern of this sample, which is shown in Figure 10d, is similar to that of the polymer-rich phase sample from the solution containing 28 wt % CO_2, indicating that only the β form was generated in the sample. Even though not included in the present article, both the FTIR and the DSC results on these samples also showed presence of only the β crystalline form. The difference in the samples generated from 28 and 43% CO_2 containing solutions is thus only in the morphological appearance and not the actual crystalline form which is the β in both cases.

5. Further Discussion on Path Dependence of the Crystalline Forms. The path dependence of the gel structures in terms of the different crystalline forms can be understood from a close examination of the phase diagrams. Figure 15 a and b are schematic representations of the T-x phase diagrams for sPS solutions in good and poor solvents at ambient pressure that is adapted from the literature.[17,33,41] In good solvents, the melting point depression of the β form is large and the melting curve intersects with the L + δ boundary. This is due to the solvent quality being good and the stability of the polymer−solvent compound (i.e., the δ form) being also improved with improved solvent quality. In good solvents, the β form is the thermodynamically stable phase at high polymer concentrations, while the helical δ form is the thermodynamically stable phase at lower polymer concentrations. At high polymer concentrations, a metastable "β + δ" region is reported at lower temperatures.

In poor solvents, with decreased solvent quality, the melting point depression is reduced, and the melting curve moves to higher temperatures. The stability of δ form is also decreased. As shown in Figure 15b, in poor solvents, the β form becomes the thermodynamically stable phase in the whole concentration range and the "L + δ" and the "β + δ" regions depicted at lower temperatures below the "L + β" region are metastable.

Figure 16 shows the schematics for the phase diagram and the phase separation paths in toluene + CO_2 mixtures at relatively high CO_2 content that we propose as being applicable at high pressures in the present study. These are based on the observations in the view cell and the results obtained from the XRD, FTIR, and SEM of the samples collected after different paths. DSC type calorimetric measurements that are generally

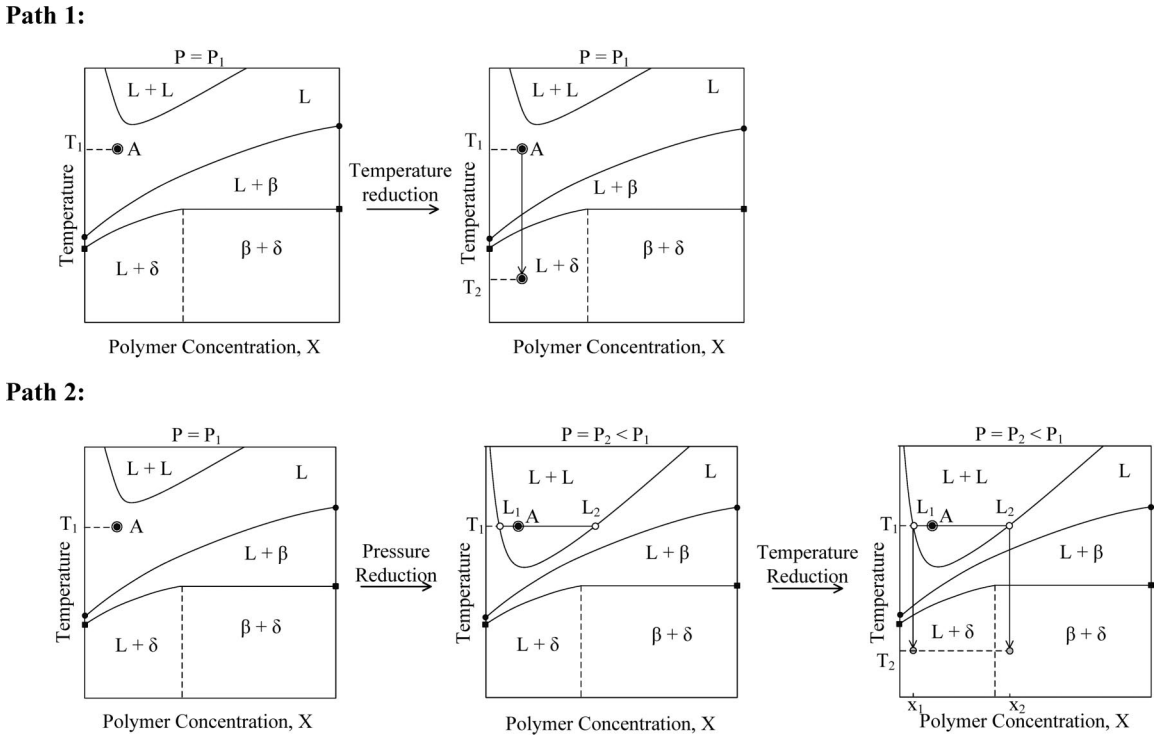

Figure 16. Schematic representation of the $T-x$ phase diagrams for sPS in toluene + CO_2 at high pressures and the consequence of paths followed on the eventual crystalline forms that are generated. P is pressure, L_1 and L_2 are the polymer-lean and the polymer-rich phases. Other symbols are as in Figure 15.

used to generate phase diagrams at ambient pressures are not experimentally amenable to high-pressure measurements in ternary systems that consist of polymer + solvent + carbon dioxide.

In proposing these figures, for simplicity, the system is further viewed as a two-component system composed of the polymer and the pseudosolvent (the mixture of toluene + CO_2). At the higher temperatures the LCST-type two phase region (L + L) is depicted which is supported by the experimental data in Figure 4. The present study shows that these fluid mixtures at high pressures indeed behave as relatively good solvents, leading to completely homogeneous solutions over a wide temperature range at all pressures investigated for mixtures containing up to 16 wt % CO_2. In the case of the system containing 28 wt % CO_2, the solvent quality becomes poorer, and at lower pressures a liquid−liquid phase separation is observed upon an increase in temperature.

The region below the homogeneous liquid (L) region is viewed to be more like the poor solvent case shown in Figure 15b, but somewhat modified to account for high pressures and the improved solvent quality that accompanies higher pressures. Thus the diagram depicts a picture that describes the system as being in an intermediate solvent. The lower temperature portion of the phase diagram is based on the SEM observations on the gel samples that we have presented in the previous sections. The micrographs of the gels formed from the mixture of toluene (72) + CO_2 (28) indicate the presence of the β form over the whole polymer concentration range. Thus, in Figure 16, the region below the homogeneous liquid phase is the L + β region corresponding to the coexistence of the solution and the β crystal phase (representing the zigzag chain conformation) over the full polymer concentration range. The L + β region is depicted as narrowing at lower polymer concentrations due to the larger melting point depression of the β crystal form with the increasing amount of the solvent in the system. Below the L + β region is L + δ region corresponding to the coexistence of the solution and the polymer-compound phase (δ phase) observed at the low polymer concentrations. There is a metastable $\beta + \delta$ region at higher polymer concentrations, where β and δ forms coexist.

As already noted, the sPS solutions in toluene + CO_2 for solutions containing 28% CO_2 also display a LCST-type L−L phase behavior in the high-temperature region. In Figure 16, along Path 1, upon reduction of temperature the homogeneous solution at point A enters the L + β region which is then followed by entry into the L + δ region where the polymer forms the polymer−solvent compound and solution undergoes gelation. Final depressurization stage to ambient pressure (see Figure 9) does not alter the structure of the compound. The samples collected through Path 1 show primarily the δ crystal form and a fibrillar morphology. Presence of a small fraction of the β form was also indicated in the SEM micrographs (Figure 13). The presence of the β form is understandable since the system traverses the narrow L + β region during the cooling process. The system experiences an early stage of crystallization that would lead to the β form. Further development of the β form is however hindered upon entering the L + δ region with continual cooling where the δ form rather than the β form is promoted.

In Figure 16, along Path 2, the homogeneous solution at point A enters the L−L phase-separated region upon reduction of pressure which moves the LCST to lower temperatures. The solution which was homogeneous at T_1 is now in the immiscible region and the system phase separates into two coexisting phases, a polymer-lean phase (L_1) and a polymer-rich phase (L_2). In the second step along Path 2 (see Figure 9) where temperature is reduced, these two phases undergo a process similar to Path 1. The polymer-rich phase enters the L + β region first and then goes into a metastable $\beta + \delta$ region, while the polymer-lean phase crosses L + β region and enters the L + δ region. For the polymer-rich phase, the rate of crystallization of the β form is promoted and progresses to completion. As shown in the figure, at higher polymer concentrations the temperature range for the stable L + β region is larger. There

Path 2:

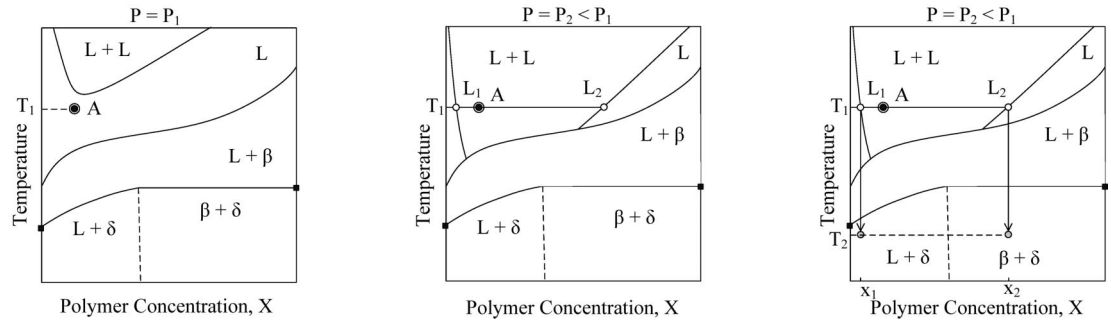

Figure 17. Schematic representation of the $T-x$ phase diagram for sPS in toluene + CO_2 with higher CO_2 content at high pressures. Symbols are as in Figure 16.

is sufficient time during the cooling process that the system remains in the L + β region which leads to the effective formation and completion of the stable zigzag β form. With further cooling, the system enters the metastable $\delta + \beta$ region, but the stable β that was generated in the higher temperature range remains with no transformation to the δ form. This is consistent with the experimental observation that only the β form was collected for the polymer-rich phase. For the polymer-lean phase L_1, during reduction of temperature to room temperature the system first enters the L + β region and then the L + δ region. One then expects the final crystal form to be predominantly the δ form with presence of a minor β component, as was the case for Path 1. This is actually in contrast to the experimental observations. What is actually observed is a mixture of $\delta + \beta$ forms with relatively large amount of β (see Figure 13d). This discrepancy may be attributed to the different level of CO_2 in the polymer-lean phase and polymer-rich phase after the L−L phase separation. In the ternary system of polymer (sPS) + good solvent (toluene) + poor solvent (CO_2), the polymer-lean phase tends to have more CO_2 compared to the polymer-rich phase after the L−L phase separation.[44] An increase in CO_2 content in the polymer-lean phase leads a decrease in the solvent quality which results in destabilization of the polymer−solvent compound (δ phase) and promotion of the formation of the β form. This would then lead to a mixture of $\beta + \delta$ forms with a relatively large amount of the β form, as is experimentally observed.

Figure 17 presents a schematic of $T-x$ diagram for sPS solution in the mixture solvent with higher (43%) CO_2. As compared to Figure 16 for the mixture solvent containing 28% CO_2, Figure 17 includes features that account for the higher reduction in solvent power. The L + β phase boundary is shifted to higher temperatures since the extent of melting point depression of β crystal form would be further decreased due to further reduction of the solvent quality. The L + δ phase boundary is shifted to lower temperatures due to decreased solvent quality. The L−L phase boundary is shifted to lower temperatures (reducing the homogeneous region) due to reduced solvent quality. As also indicated in the $T-P$ phase diagram shown in Figure 4, the LCST type L−L phase boundary shifts to higher pressures with increasing the CO_2 content in the solvents. This actually leads to a deeper pressure quench below the phase boundary for the solvent with 43 wt % CO_2 compared to the solution with 28 wt % CO_2 even when the same pressure jump (~35 MPa) is imposed.

The $T-x$ diagram corresponding to a lower pressure P_2 is also shown in Figure 17. The solution which was homogeneous at point A at P_1 when pressure is lowered to P_2 undergoes phase separation into the polymer-rich and the polymer-lean phases that coexist. Due to the deeper pressure quench experienced in this higher CO_2 containing solution, the polymer-rich phase at L_2 has a higher polymer concentration, and the polymer-lean phase at L_1 has a lower polymer content compared with that in Figure 16 depicting the case for the lower CO_2 containing solution. Further cooling from L_2 leads to the crystallization in the β form from polymer-rich phase at this high polymer concentration resulting in the denser spherulitic structures that were observed in Figure 14. The polymer-lean phase L_1 has extremely low polymer content which prevented sampling for characterization. But Figure 17 would suggest that if a sample could have been collected the polymer in the polymer-lean phase it would also have been dominated by the β crystal form.

The relative amount of the β form and the crystal morphology observed in the SEM of the different samples can be viewed as reflecting the different stages of the crystallization of the β form. The small β crystal domains dispersed within fibrillar network formed from sPS solutions in toluene (72) + CO_2 (28) through Path 1, which could only be observed in SEM micrograph and not detected in XRD and FTIR measurement, may be regarded as reflecting the early stage of crystallization, the further growth of which is prevented due to entry into the L + δ region where the δ form is promoted instead. The β crystal morphology observed in the polymer-rich phase obtained from sPS solutions in toluene (72) + CO_2 (28) through Path 2 may be viewed to represent the middle stage of crystallization in which higher crystallization rates and longer crystallization times permit the development of the lamellar disks. The β crystal morphology observed in samples collected from the polymer-rich phase generated from sPS solutions through Path 2 in toluene + CO_2 with higher amount of CO_2 (43 wt %) may be viewed as reflecting the late stage of crystallization. The higher supersaturation and crystallization rate and longer crystallization time available in the wider L + β region lead to the formation of denser, spherulitic structures.

Conclusions

Only the sol−gel phase boundary was observed in solutions of sPS in pure toluene and toluene + CO_2 mixtures up to 16 wt % CO_2. In solutions with more than 28 wt % CO_2, both sol−gel and liquid−liquid phase separations were observed. The liquid−liquid phase boundary shifted to higher pressures with increasing amount of CO_2 in the solution. The gel samples formed from the sPS solutions in pure toluene and toluene + CO_2 with a CO_2 level up to 16 wt % show a fibrillar network morphology with δ crystal structure. The sPS samples collected from the solutions with higher level of CO_2, i.e., 28 wt % CO_2 in solvent mixture, depending upon the paths followed, are found to display different crystalline structures and morphological feature. The samples collected through constant pressure cooling show a fibrillar structure with a small portion of β form, while the system containing high level of CO_2 first undergoes L−L

phase separation by constant temperature pressure quench. The samples recovered after the L−L phase separation show different structures. For the polymer-rich phase, the samples show stacked-lamellar morphology and the β form crystalline structure, and for the polymer-lean phase, the morphology is that of lamellar layers connected with fine fibers displaying a mixture of δ and β phase crystalline structures. With even higher CO_2 content in system, i.e., 43 wt % in solvent mixture, samples collected from polymer-rich phase display a denser stacked-lamellar morphology with spherulitic attributes and β crystalline structure.

References and Notes

(1) Malanga, M. *Adv. Mater.* **2000**, *12*, 1869–1872.
(2) Guerra, G.; Vitagliano, V. M.; De Rosa, C.; Petraccone, V.; Corradini, P. *Macromolecules* **1990**, *23*, 1539–1544.
(3) De Rosa, C.; Rapacciuolo, M.; Guerra, G.; Petraccone, V.; Corradini, P. *Polymer* **1992**, *33*, 1423–1428.
(4) Chatani, Y.; Shimane, Y.; Ljitsu, T.; Yukinari, T. *Polymer* **1993**, *34* (8), 1620–1624.
(5) Manfredi, C.; De Rosa, C.; Guerra, G.; Rapacciuolo, M.; Auriemma, F.; Corradini, P. *Macromol. Chem. Phys.* **1995**, *196*, 2795–2808.
(6) Reverchon, E.; Venditto, V. *J. Appl. Polym. Sci.* **1999**, *74*, 2077–2082.
(7) Rizzo, P.; Daniel, C.; De Girolamo Del Mauro, A.; Guerra, G. *Chem. Mater.* **2007**, *19*, 3864–3866.
(8) Petraccone, V.; Ruiz de Ballesteros, O.; Tarallo, O.; Rizzo, P.; Guerra, G. *Chem. Mater.* **2008**, *20* (11), 3663–3668.
(9) Vittoria, V.; De Candia, F.; Iannelli, P.; Immirzi, A. *Makromol. Chem., Rapid Commun.* **1988**, *9*, 765–769.
(10) Immirzi, A.; De Candia, F.; Iannelli, P.; Zambelli, A.; Vittoria, V. *Makromol. Chem., Rapid Commun.* **1988**, *9*, 761–764.
(11) Rapacciuolo, M.; De Rosa, C.; Guerra, G.; Mensitieri, G.; Apicella, A.; Del Nobile, M. A. *J. Mater. Sci. Lett.* **1991**, *10*, 1084–1087.
(12) Handa, P. Y.; Zhang, Z.; Wong, B. *Macromolecules* **1997**, *30*, 8499–8504.
(13) Ma, W.; Yu, J.; He, J. *Macromolecules* **2004**, *37*, 6912–6917.
(14) Daniel, C.; Menelle, A.; Brulet, A.; Guenet, J.-M. *Polymer* **1996**, *37*, 1273–1280.
(15) Daniel, C.; Menelle, A.; Brulet, A.; Guenet, J.-M. *Polymer* **1997**, *38*, 4193–4199.
(16) De Rudder, J.; Berghmans, H.; De Schryver, F. C.; Bosco, M.; Paoletti, S. *Macromolecules* **2002**, *35*, 9529–9535.
(17) Deberdt, F.; Berghmans, H. *Polymer* **1993**, *34*, 2192–2201.
(18) Deberdt, F.; Berghmans, H. *Polymer* **1994**, *35*, 1694–1704.
(19) Guenet, J.-M. *Thermoreversible gelation of polymers and biopolymers*; Academic Press: London, 1992.
(20) Clark, A. H.; Ross-Murphy, S. B. *Adv. Polym. Sci.* **1987**, *83*, 57–192.
(21) te Nijenhuis, K. *Adv. Polym. Sci.* **1997**, *130*, 1.
(22) Li, Y.; Xue, G. *Macromol. Rapid Commun.* **1998**, *19*, 549–552.
(23) Daniel, C.; Alfano, D.; Venditto, V.; Cardea, S.; Reverchon, E.; Larobina, D.; Mensitieri, G.; Guerra, G. *Adv. Mater.* **2005**, *17*, 1515–1518.
(24) Roels, T.; Deberdt, F.; Berghmans, H. *Macromolecules* **1994**, *27*, 6216–6220.
(25) Roels, T.; Rastogi, S.; De Rudder, J.; Berghmans, H. *Macromolecules* **1997**, *30*, 7939–7944.
(26) Gu, M.; Zhang, J.; Wang, X.; Tao, H.; Ge, L. *Desalination* **2006**, *192*, 160–167.
(27) Li, D.; Krantz, W. B.; Greensberg, A. R.; Sani, R. L. *J. Membr. Sci.* **2006**, *279*, 50–60.
(28) Yave, W.; Quijada, R.; Ulbricht, M.; Benavente, R. *Polymer* **2005**, *46*, 11582–11590.
(29) Zhang, W.; Kiran, E. *J. Supercrit. Fluids* **2006**, *38*, 406–419.
(30) Ray, B.; Elhasri, S.; Thierry, A.; Marie, P.; Guenet, J.-M. *Macromolecules* **2002**, *35*, 9730–9736.
(31) Fang, J.; Kiran, E. *J. Supercrit. Fluids* **2006**, *38*, 132–145.
(32) Kiran, E.; Liu, K. *Korean J. Chem. Eng.* **2002**, *19*, 153–158.
(33) Berghmans, H.; Deberdt, F. *Philos. Trans. R. Soc. London A* **1994**, *348*, 117–130.
(34) Kitts, C. C.; Vanden Bout, D. A. *Polymer* **2007**, *48*, 2322–2330.
(35) Zhang, W.; Dindar, C.; Bayraktar, Z.; Kiran, E. *J. Appl. Polym. Sci.* **2003**, *89*, 2201–2209.
(36) Gowd, E. B.; Nair, S. S.; Ramesh, C.; Tashiro, K. *Macromolecules* **2003**, *36*, 7388–7397.
(37) Reynolds, N. M.; Savage, J. D.; Hsu, S. L. *Macromolecules* **1989**, *22*, 2867–2869.
(38) Yoshioka, A.; Tashiro, K. *Macromolecules* **2003**, *36*, 3001–3003.
(39) Moyses, S.; Spells, S. J. *Macromolecules* **1999**, *32*, 2684–2689.
(40) Kobayashi, M.; Nakaoki, T.; Ishihara, N. *Macromolecules* **1989**, *22*, 4377–4382.
(41) Rastogi, S.; Goossens, J. G. P.; lemstra, P. J. *Macromolecules* **1998**, *31*, 2983–2998.
(42) Chatani, Y.; Shimane, Y.; Inoue, Y.; Inagaki, T.; Ishioka, T.; Ijitsu, T.; Yukinari, T. *Polymer* **1992**, *33*, 488–492.
(43) Galdi, N.; Albunia, A. R.; Oliva, L.; Guerra, G. *Macromolecules* **2006**, *39*, 9171–9176.
(44) Kiran, E. Polymer formation, modification and processing in or with supercritical fluids. In *Supercritical Fluids*; Kiran, E., Levelt Sengers, J. M. H., Eds.; Kluwer Academic Publishers: Dordrecht, The Netherlands, 1994; pp 541−588.

MA801511C